

REPORT 936

DESIGN AND PERFORMANCE OF FAMILY OF DIFFUSING SCROLLS WITH MIXED-FLOW IMPELLER AND VANELESS DIFFUSER

By W. BYRON BROWN and GUY R. BRADSHAW

SUMMARY

A family of diffusing scrolls was designed for use with a mixed-flow impeller and a small-diameter vaneless diffuser. The design theory, intended to maintain a uniform pressure around the scroll inlet, permits determination of the position of scroll cross sections of preassigned area by considering the radial variation in fluid density and the effects of friction along the scroll. Inasmuch as the design method leaves the cross-sectional shape undetermined, the effect of certain variations in scroll shape was investigated by studying scrolls having angles of divergence (of the scroll walls downstream of the entrance section) of 24° , 40° , and 80° . A second 80° scroll was of asymmetrical construction and a third was plaster-cast instead of sand-cast. Each scroll was tested as a compressor component at actual impeller tip speeds of 700 to 1300 feet per second from full throttle to surge.

The changes in scroll geometry and in surface condition employed in this study had only unimportant effects on compressor performance, although some evidence existed that the 24° divergence angle was too small for optimum performance at the highest tip speeds. With this possible exception, the results indicated that the design method is applicable over the range of scroll shapes investigated.

Comparison of over-all compressor performance, using the same impeller and various diffuser-collector combinations, showed the performance of a 20-inch vaneless diffuser and scroll to be approximately the same as that of a 34-inch vaneless diffuser and collector ring and to have higher efficiency and pressure coefficient than a 17-inch vaned diffuser and collector ring. Substitution of the scroll for the collector ring, with the 20-inch vaneless diffuser, resulted in substantial increases in efficiency and pressure coefficient, and in an extension of the operating range to higher values of load coefficient.

INTRODUCTION

A survey of unpublished data on compressor performance with both vaned and vaneless diffusers using the same impeller suggests the possibility of combining the desirable characteristics of the two types of diffuser and thus increasing the adaptability and the performance of centrifugal compressors. The vaneless diffuser has the advantage of a relatively wide operating range at reasonably high efficiencies because of freedom from blade stalling and absence of shock waves from guide vanes. This advantage, however, is accompanied by a serious penalty in size; the vaneless diffuser

is considerably larger than the vaned diffuser that gives equivalent energy conversion.

Examination of unpublished available data on the relation between vaneless-diffuser diameter and compressor performance indicated that the decrease in vaneless-diffuser efficiency with reduction in size was approximately proportional to kinetic-energy losses at the inlet to a conventional collector ring, and that the substitution of a diffusing scroll for the collector ring might reduce these losses to the point where a small-diameter vaneless diffuser could be efficiently employed.

In order to investigate the possibilities of this combination, a family of five scrolls was designed for use with a 20-inch-diameter vaneless diffuser. The design theory, suggested by William Bollay in a Pratt & Whitney report, determines the circumferential location of a given cross-sectional area but does not fix the geometry of the scroll. During 1945, an experimental investigation was therefore undertaken at the NACA Cleveland laboratory to study the validity of the design theory, to examine the permissible variations in certain form parameters, to study the effect of these variations on compressor performance, and to determine the effect of a diffusing scroll on vaneless-diffuser performance.

The method employed in designing the scrolls is described and the experimental results obtained with the five different scrolls are presented. Compressor-performance curves also compare the performance of the same impeller used with (a) the manufacturer's vaned diffuser, (b) a 20-inch vaneless diffuser, (c) a 34-inch-diameter vaneless diffuser—each with the same collector ring, and (d) the 20-inch vaneless diffuser with a diffusing scroll.

SYMBOLS

The following symbols are used in this report:

b	width of scroll passage at any radius normal to center line of diffuser (fig. 1), inches
c_p	specific heat at constant pressure, foot-pounds per pound $^\circ\text{F}$
D	impeller-outlet diameter, feet
F	coefficient used in scroll calculations
f	friction factor
g	acceleration of gravity, 32.174 feet per second per second
I_x, I_y, I_z	abbreviations used for integrals in scroll calculations

the change of state of the fluid is assumed to be reversible and adiabatic. The analysis is thereby simplified and, inasmuch as the radial-density ratio across any one section of the scroll (isentropic compression assumed) was found to have a maximum value of about 1:1.1, the error introduced by neglecting friction is negligibly small. The effects of friction cannot, of course, be ignored in calculating the location of the chosen cross sections from the equation of angular momentum.

RADIAL VARIATION IN DENSITY

By combining the isentropic equation

$$\left(\frac{\rho}{\rho_i}\right)^{\gamma-1} = \frac{t}{t_i}$$

and the relation between total and static temperatures

$$T = t_i + \frac{V_i^2}{2gc_p} = t + \frac{V^2}{2gc_p}$$

the density ratio may be written in the form

$$\frac{\rho}{\rho_i} = \left[1 + \frac{1}{2gc_p t_i} (V_i^2 - V^2) \right]^{\frac{1}{\gamma-1}} \quad (1)$$

Equation (1) may be so modified as to give the density ratio in terms of inlet conditions and geometrical constants of the scroll. The continuity equation provides the relation

$$\rho b r d\phi V_r = \rho_i b_i r_i d\phi V_{r,i}$$

$$V_r = V_{r,i} \frac{\rho_i b_i r_i}{\rho b r}$$

where r is the distance to the midpoint of b .

If the effect on V_r of the density change is now assumed negligible compared with the effect produced by changes in r and b , the equation becomes

$$V_r = V_{r,i} \frac{b_i r_i}{b r} \quad (2)$$

When friction is neglected in the determination of the radial variation in density (isentropic-state change), the principle of conservation of angular momentum gives for the tangential component of the velocity

$$V_\theta = V_{\theta,i} \frac{r_i}{r} \quad (3)$$

Rewriting equation (1) in terms of radial and tangential velocity components and substituting the values of V_r and V_θ from equations (2) and (3) yield

$$\frac{\rho}{\rho_i} = \left\{ 1 + \frac{1}{2gc_p t_i} \left[V_{\theta,i}^2 \left(1 - \frac{r_i^2}{r^2} \right) + V_{r,i}^2 \left(1 - \frac{b_i^2 r_i^2}{b^2 r^2} \right) \right] \right\}^{\frac{1}{\gamma-1}} \quad (4)$$

Equation (4) gives an expression for the density at any radius, under the preceding assumptions, in terms of scroll-

inlet conditions and geometric constants of the scroll that are known as soon as the cross-sectional shape has been chosen.

CIRCUMFERENTIAL LOCATION OF CHOSEN CROSS SECTIONS OF SCROLL

For flow through the scroll, the equation of continuity gives

$$\rho_i b_i V_{r,i} r_i \phi = \int_{r_i}^{r_{max}} \rho b V_\theta \epsilon dr \quad (5)$$

In determining the radial variation of the tangential component of the velocity, the effect of friction is considered by assuming that

$$\frac{V_\theta}{V_{\theta,i}} = \frac{r_i}{r} - \sigma \left(\frac{r}{r_i} - 1 \right) \quad (6)$$

The index σ is closely proportional to the friction coefficient over a short distance but changes slowly through the scroll. Its value is fixed by the condition that the equations of continuity and angular momentum be satisfied simultaneously. Inasmuch as the actual design procedure is a step-by-step process, σ is assumed constant only over a single segment of the scroll and may take a new value for the next segment.

From equations (5) and (6)

$$\phi = \frac{V_{\theta,i}}{V_{r,i}} \int_{r_i}^{r_{max}} \frac{\rho}{\rho_i} \frac{b}{b_i} \frac{r}{r_i} \epsilon dr \left[\frac{r_i}{r} - \sigma \left(\frac{r}{r_i} - 1 \right) \right] \quad (7)$$

If equation (7) is rearranged and r/r_i is set equal to x ,

$$\phi = \frac{V_{\theta,i}}{V_{r,i}} \left[\int_1^{x_{max}} \frac{\rho}{\rho_i} \frac{b}{b_i} \frac{\epsilon dx}{x} - \sigma \int_1^{x_{max}} \frac{\rho}{\rho_i} \frac{b}{b_i} (x-1) \epsilon dx \right] \quad (8)$$

The abbreviations

$$\left. \begin{aligned} I_x &= \frac{V_{\theta,i}}{V_{r,i}} \int_1^{x_{max}} \frac{\rho}{\rho_i} \frac{b}{b_i} \frac{\epsilon dx}{x} \\ I_y &= \frac{V_{\theta,i}}{V_{r,i}} \int_1^{x_{max}} \frac{\rho}{\rho_i} \frac{b}{b_i} (x-1) \epsilon dx \end{aligned} \right\} \quad (9)$$

give equation (8) the form

$$\phi = I_x - \sigma I_y \quad (10)$$

A second equation in ϕ and σ is required. This equation can be obtained from a consideration of the loss in angular momentum due to friction, expressed in terms of the torque on the segment between adjacent cross sections. Because of friction, the torque per unit length

$$M = - \int \tau dl r$$

Inasmuch as neither τ nor r changes greatly over a segment, mean values may be used and

$$M = - \bar{\tau} \bar{r} f dl \quad (11)$$

where the bar indicates the mean value found from the relation

$$\bar{r} = \frac{\int_{r_1}^{r_{\max}} r dl}{l}$$

The applied torque due to surface friction over the segment between sections 1 and 2 in the volute (half scroll) M_{1-2} can be written as

$$M_{1-2} = -\frac{\bar{\tau}_1 \bar{r}_1 l_1 + \bar{\tau}_2 \bar{r}_2 l_2}{2} \frac{\bar{r}_1 + \bar{r}_2}{2} (\phi_2 - \phi_1) \quad (12)$$

Because $\tau = \frac{f}{2} \rho V_{\theta}^2$, equation 12 may be written

$$M_{1-2} = -\frac{f}{8} (\bar{r}_1 + \bar{r}_2) (\bar{V}_{\theta,1}^2 \bar{\rho}_1 \bar{r}_1 l_1 + \bar{V}_{\theta,2}^2 \bar{\rho}_2 \bar{r}_2 l_2) (\phi_2 - \phi_1)$$

The values for $\bar{V}_{\theta,1}$ and $\bar{V}_{\theta,2}$ obtained from equation (3) instead of equation (6) may be inserted in this equation and result in considerable simplification without introducing appreciable error. This substitution, using a mean value of density for the segment $\bar{\rho}_{1-2}$, and rearrangement allow this equation to be put in the form

$$M_{1-2} = -F_{1-2} \rho_t V_{\theta,t}^2 r_t^2 b_t (\phi_2 - \phi_1) \quad (13)$$

where

$$F_{1-2} = \frac{f}{8} \frac{\bar{\rho}_{1-2}}{\rho_t} \frac{1}{b_t} \left(\frac{l_1}{\bar{r}_1} + \frac{l_2}{\bar{r}_2} \right) (\bar{r}_1 + \bar{r}_2) \quad (14)$$

The outflow of angular momentum per second through the second section is

$$\int_{r_2}^{r_{\max}} \rho_2 V_{\theta,2}^2 b_2 r_2 \epsilon dr$$

This expression is equal to the inflow from the first section,

$$\int_{r_1}^{r_{\max}} \rho_1 V_{\theta,1}^2 b_1 r_1 \epsilon dr$$

plus the inflow across the periphery of the second segment,

$$\rho_t b_t V_{r,t} V_{\theta,t} r_t^2 (\phi_2 - \phi_1)$$

minus the torque loss in the second segment due to friction M_{1-2} ; that is,

$$\int_{r_2}^{r_{\max}} \rho_2 V_{\theta,2}^2 b_2 r_2 \epsilon dr = \int_{r_1}^{r_{\max}} \rho_1 V_{\theta,1}^2 b_1 r_1 \epsilon dr + (\rho_t b_t V_{r,t} V_{\theta,t} r_t^2 - F_{1-2} \rho_t V_{\theta,t}^2 r_t^2 b_t) (\phi_2 - \phi_1) \quad (15)$$

When equation (15) is solved for ϕ_2

$$\left(1 - F_{1-2} \frac{V_{\theta,t}}{V_{r,t}} \right) \phi_2 = \frac{1}{V_{\theta,t} V_{r,t}} \int_{r_1}^{r_{\max}} \frac{\rho_2 b_2 r_2 \epsilon dr}{\rho_t b_t r_t} V_{\theta,2}^2 - \frac{1}{V_{\theta,t} V_{r,t}} \int_{r_2}^{r_{\max}} \frac{\rho_1 b_1 r_1 \epsilon dr}{\rho_t b_t r_t} V_{\theta,1}^2 - F_{1-2} \frac{V_{\theta,t}}{V_{r,t}} \phi_1 + \phi_1 \quad (16)$$

If the value of V_{θ} from equation (6) is substituted, if $x = r/r_t$

is used, and if the quantities under the integral sign are rearranged, the expression

$$\frac{1}{V_{\theta,t} V_{r,t}} \int_{r_1}^{r_{\max}} \frac{\rho_2 b_2 r_2 \epsilon dr}{\rho_t b_t r_t} V_{\theta,2}^2$$

may be put in the form

$$\frac{V_{\theta,t}}{V_{r,t}} \left[\int_1^{x_{\max}} \frac{\rho_2 b_2 \epsilon dx}{\rho_t b_t x} - 2\sigma_2 \int_1^{x_{\max}} \frac{\rho_2 b_2}{\rho_t b_t} (x-1) \epsilon dx + \sigma_2^2 \int_1^{x_{\max}} \frac{\rho_2 b_2}{\rho_t b_t} x(x-1)^2 \epsilon dx \right]$$

with a similar expression in ρ_1 and b_1 for the second integral. Using equation (8) and the additional abbreviation

$$I_{x,2} = \frac{V_{\theta,t}}{V_{r,t}} \int_1^{x_{\max}} \frac{\rho}{\rho_t} \frac{b}{b_t} x(x-1)^2 \epsilon dx \quad (17)$$

allows the expression to be put into the form

$$I_{x,2} - 2\sigma_2 I_{y,2} + \sigma_2^2 I_{z,2}$$

where the second subscript identifies the scroll segment under consideration. Equation (16) then takes the form

$$\left(1 - F_{1-2} \frac{V_{\theta,t}}{V_{r,t}} \right) \phi_2 = I_{x,2} - 2\sigma_2 I_{y,2} + \sigma_2^2 I_{z,2} - I_{x,1} + 2\sigma_1 I_{y,1} - \sigma_1^2 I_{z,1} + \left(1 - F_{1-2} \frac{V_{\theta,t}}{V_{r,t}} \right) \phi_1 \quad (18)$$

For the first segment of the scroll, between the tongue and the first cross section,

$$\phi_0 = I_{x,0} = I_{y,0} = I_{z,0} = 0$$

from which it follows that

$$\left(1 - F_{0-1} \frac{V_{\theta,t}}{V_{r,t}} \right) \phi_1 = I_{x,1} - 2\sigma_1 I_{y,1} + \sigma_1^2 I_{z,1} \quad (19)$$

If equation (19) is substituted in equation (18)

$$\begin{aligned} \left(1 - F_{1-2} \frac{V_{\theta,t}}{V_{r,t}} \right) \phi_2 &= I_{x,2} - 2\sigma_2 I_{y,2} + \sigma_2^2 I_{z,2} - \\ &\left(1 - F_{0-1} \frac{V_{\theta,t}}{V_{r,t}} \right) \phi_1 + \left(1 - F_{1-2} \frac{V_{\theta,t}}{V_{r,t}} \right) \phi_1 \\ &= I_{x,2} - 2\sigma_2 I_{y,2} + \sigma_2^2 I_{z,2} - (F_{1-2} - F_{0-1}) \frac{V_{\theta,t}}{V_{r,t}} \phi_1 \end{aligned} \quad (20)$$

In general, then, for the n th segment,

$$\begin{aligned} \left(1 - F_{(n-1)-n} \frac{V_{\theta,t}}{V_{r,t}} \right) \phi_n &= I_{x,n} - 2\sigma_n I_{y,n} + \sigma_n^2 I_{z,n} - \\ &(F_{(n-1)-n} - F_{(n-2)-(n-1)}) \phi_{n-1} \frac{V_{\theta,t}}{V_{r,t}} - \\ &(F_{(n-2)-(n-1)} - F_{(n-3)-(n-2)}) \phi_{n-2} \frac{V_{\theta,t}}{V_{r,t}} \dots - \\ &(F_{1-2} - F_{0-1}) \phi_1 \frac{V_{\theta,t}}{V_{r,t}} \end{aligned} \quad (21)$$

DESIGN PROCEDURE FOR DIFFUSING SCROLLS

The area at the scroll outlet can be approximately calculated from the continuity equation. Intermediate areas, between the scroll outlet and the tongue, of any desired number and size can then be arbitrarily chosen and the circumferential location determined. Because the design theory requires specification of the cross-sectional area but not the form of the scroll, a rather wide range of geometrical shapes was employed in the experimental investigation. After a definite scroll shape had been chosen, the following design procedure was used:

1. The cross-sectional shape of the scroll was chosen.
2. From the geometry of the selected scroll shape, the values of b and x that corresponded to the preselected cross-sectional areas of the scroll were found.
3. The value of ρ/ρ_t was calculated from the design conditions at the diffuser outlet by equation (4). (If desired, a curve may be plotted giving ρ/ρ_t as a function of r/r_t .)
4. The three integrals I_x , I_y , and I_z were calculated from equations (9) and (17) for each section. In order to simplify the procedure, curves were plotted for these integrands and graphically integrated (fig. 3).

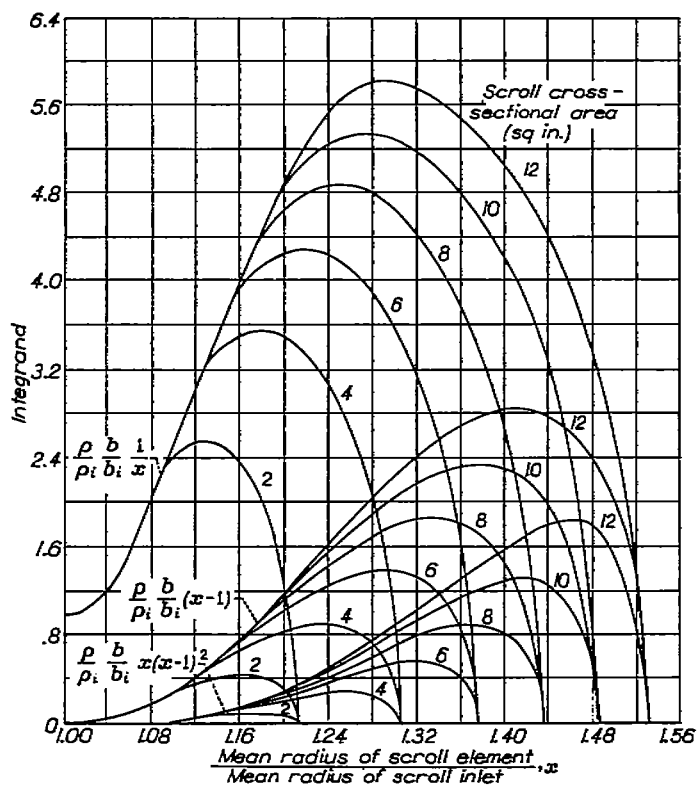


Figure 3.—Typical integrands for calculating location of different scroll sections.

5. From equation (14), the value of $F_{(n-1)-n}$ was calculated for successive segments of the scroll, starting from the tongue.
6. Values of ϕ and σ were found for successive cross sections from equations (10) and (21) by using the appropriate value for n ($n=1, 2, 3, \dots$) for each station. Curves were then drawn giving the relation between the dimensions of each section and the angle ϕ (fig. 4). (The value for $f=0.008$ shown in fig. 4 was taken from appropriate pipe-flow data.)

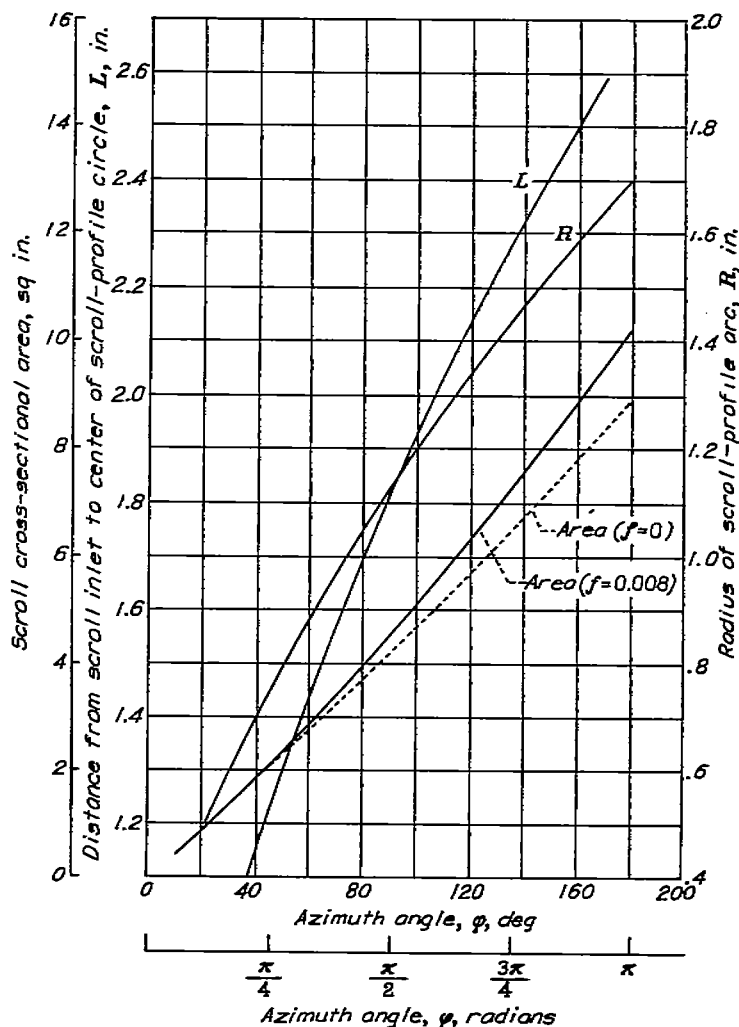


FIGURE 4.—Relation between dimensions of scroll sections and peripheral angle.

APPARATUS AND EXPERIMENTAL PROCEDURE

Impeller and diffusers.—The blades of the mixed-flow impeller used in this investigation have a gradual curvature throughout their entire length instead of the more conventional, sharply curved inducer section at the inlet. The impeller is semishrouded and has a maximum diameter of 11.24 inches; the air leaves it at an angle of 30° with a plane normal to the impeller axis. Because of space restrictions, this angle was gradually changed to 25° in the diffuser.

The diffusers, having diameters of 34 and 20 inches, are vaneless and the same except for size; the 20-inch was formed simply by cutting down the 34-inch diffuser to the desired diameter. They have a design rate of area expansion equal to that of a 6° cone and were designed by methods described in reference 1.

Diffusing scrolls.—Double scrolls were used in this study, each subtending an angle of 180° (fig. 2). By means of circular arcs, the throat of the scroll is faired into a trapezoidal cross section (as seen in a plane through the impeller axis), which in all cases but one is symmetrical about the center line of the diffuser. This trapezoidal cross section is closed at the outer end by another circular arc. The angle between the diverging walls is used to identify the scrolls. Angles of

80°, 24°, and 40° were used in this study. Scroll cross sections are shown in figure 5. One 80° scroll was so constructed that the center line of the diffuser was parallel to one wall of the scroll (fig. 5 (a)). This scroll was constructed to examine the possibility that the asymmetrical distribution of area might reduce secondary flows to a single vortex, instead of two vortices, and so decrease frictional losses in the scrolls. Another 80° symmetrical scroll was cast in plaster instead of sand in an attempt to produce a somewhat smoother surface. All the other scrolls were sand-cast. Five scrolls were studied: 80° symmetrical; 80° asymmetrical; 80° symmetrical, plaster-cast; 40° symmetrical; and 24° symmetrical. The final section of the scrolls was faired

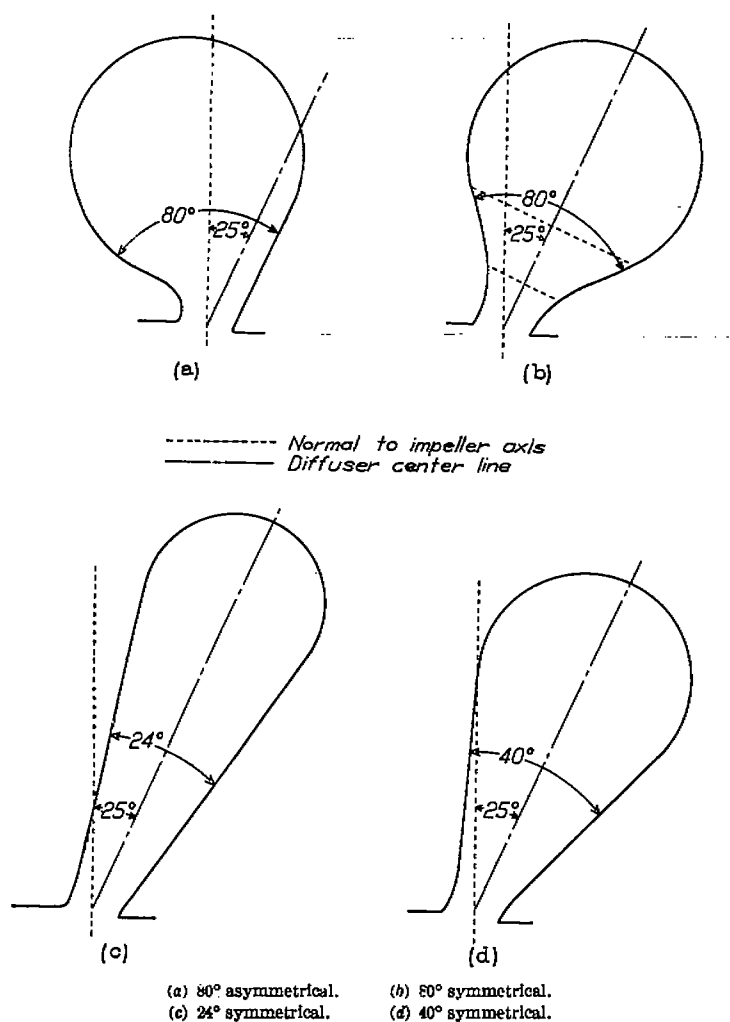


FIGURE 5.—Cross sections of scrolls.

into the outlet pipe with a rate of area expansion equivalent to that of a 6° cone throughout.

Design conditions for the scrolls, chosen to correspond with optimum impeller operating conditions, were: Air density, 0.0750 pound per cubic foot; volume flow, 72.33 cubic feet per second; total temperature at scroll inlet, 689° R; circumferential component of air velocity, 359 feet per second.

Experimental setup.—The compressor was driven by a 1000-horsepower dynamometer through a variable-speed

magnetic coupling and a step-up gearbox. A speed strip in combination with a stroboscopic tachometer operating on line frequency was used in maintaining a constant speed. A flat-plate orifice installed at the inlet to a large orifice tank was used to measure the flow. The compressor and the inlet and outlet ducts were heavily insulated to reduce heat transfer.

Standard instrumentation (reference 2) was installed for the determination of compressor over-all performance. Additional pressure measurements were taken at the diffuser outlet and inside the scroll. The location of these pressure instruments in the scroll inlet is shown in figure 2. These scroll-inlet instruments, together with the wall static-pressure taps near the outer boundary of the scroll, provided a method of verifying the design assumption that the compression was practically isentropic and that the pressure around the scroll inlet was essentially constant.

Experimental procedure.—The recommended procedure for investigating centrifugal compressors (reference 2) was followed. Runs were made at actual impeller tip speeds of 700 to 1300 feet per second, at intervals of 100 feet per second, from full throttle to surge. All the runs were made at ambient inlet-air temperature and with the collector discharging into the laboratory exhaust system. The unit was throttled at both inlet and outlet and, whenever possible, outlet pressure was maintained at 10 inches of mercury above atmospheric.

RESULTS AND DISCUSSION

COMPARISON OF PERFORMANCE OF SCROLLS

Performance characteristics of the compressor with each of the scrolls are shown in figures 6 and 7. In general, only small variations in compressor performance result from the differences in scroll geometry employed in this study. Peak efficiencies (fig. 6) are about the same for all the scrolls and occur at approximately the same load coefficient. The manner in which the efficiency drops off as maximum load coefficient is approached differs slightly, but there is no obvious relation between these variations and the modifications in scroll shape. At a tip speed of 1300 feet per second, the 24° scroll shows slightly but consistently lower efficiencies and exhibits a tendency to choke at slightly lower values of load coefficient than the other scrolls.

Pressure ratios of the compressor with each of the scrolls at actual tip speeds of 700 to 1300 feet per second are shown in figure 7. The pressure ratios for all the scrolls are essentially the same although there is again some evidence that at the higher tip speeds the 24° scroll is slightly less effective than the others. Comparison of the performance characteristics of all the scrolls indicates that, with the possible exception of the 24° scroll, all are within the applicable range of this design theory.

The circumferential distribution of static pressure at the scroll inlet is shown in figure 8 for the design flow and for maximum and minimum flows at a tip speed of 1000 feet per second. At design flow, the pressure is essentially constant; the design method therefore appears to give the required

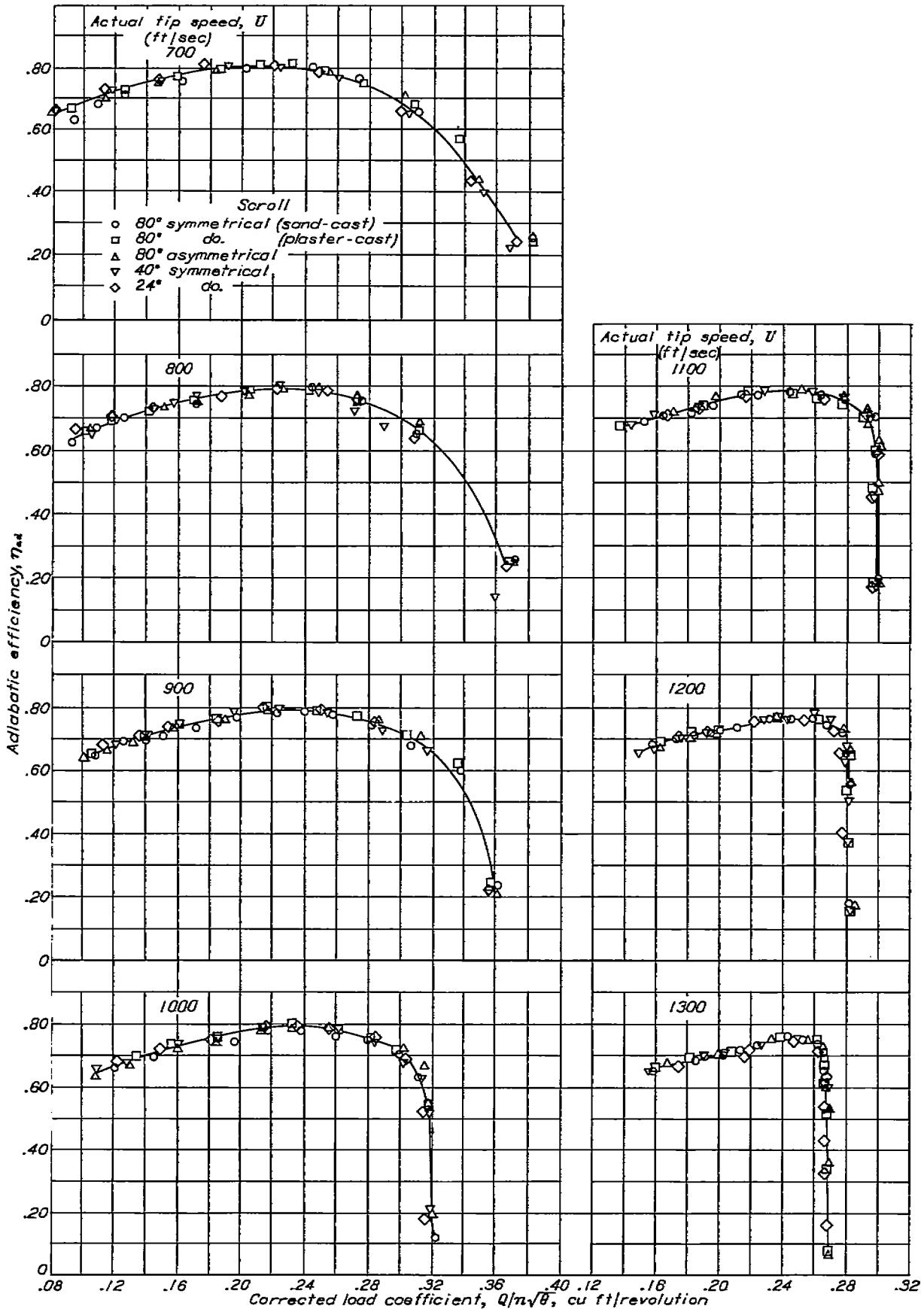


FIGURE 6.—Adiabatic efficiency of compressor with different scrolls at actual tip speeds of 700 to 1300 feet per second.

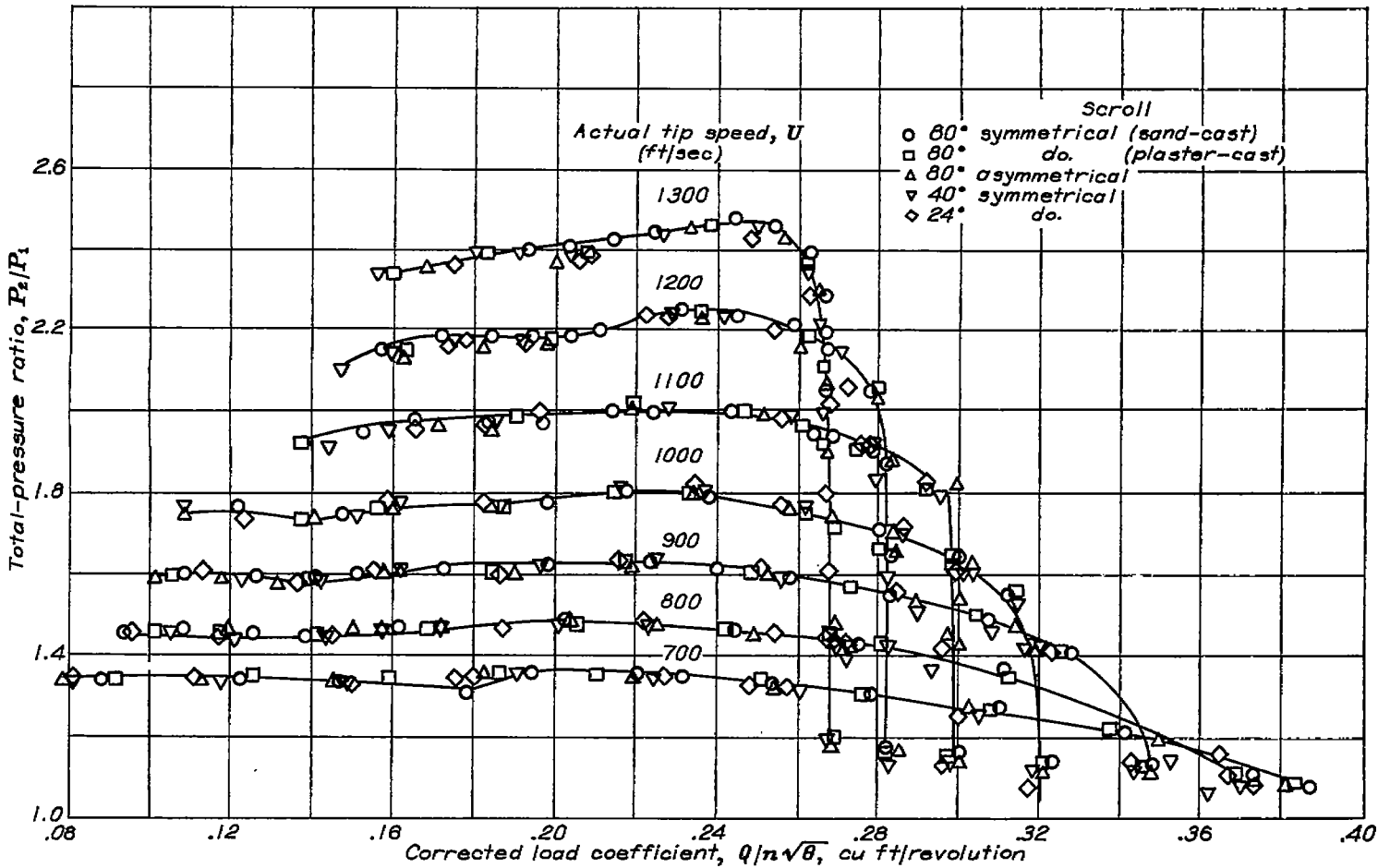


FIGURE 7.—Total-pressure ratio of compressor with different scrolls at actual tip speeds of 700 to 1300 feet per second.

pressure uniformity around the scroll inlet. At maximum flow, the static pressure at the scroll inlet decreases continuously as the angular distance from the tongue increases because the necessary velocity in the scroll requires conver-

sion of static pressure to dynamic pressure. At minimum flow, the pressure increases around the scroll inlet, showing a higher rate of diffusion along the scroll than at design flow.

The assumption of a radial-density ratio of 1:1.1 from the inlet to the outer boundary of the scroll was investigated by taking static-pressure readings near the outer periphery of the scroll. The maximum density ratio at design conditions was found to be about 1:1.07; hence, no appreciable error is introduced by assuming an isentropic change of state for design computations.

The characteristic curves for the compressor, on recommended coordinates (reference 3), are given in figure 9 for the sand-cast 80° symmetrical scroll. Because the variations in compressor performance with the different scrolls were slight, these performance curves may be considered representative of all the scrolls.

COMPARISON OF PERFORMANCE OF VARIOUS COMPRESSOR CONFIGURATIONS

Unpublished data were available from experiments in which the type of impeller used in this investigation was run with: (1) the vaned diffuser designed by the manufacturer

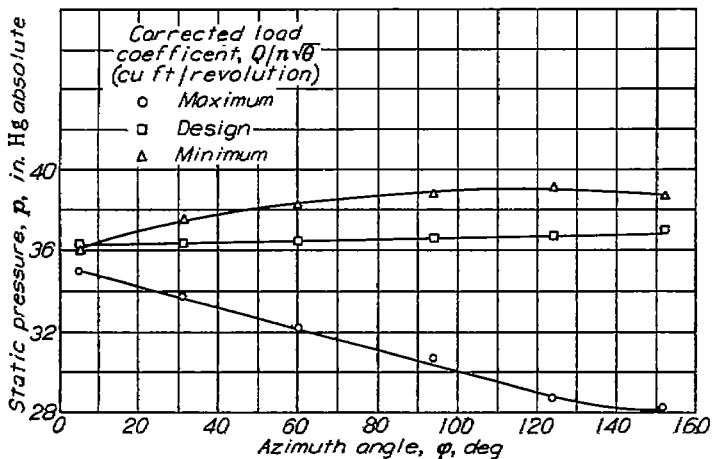


FIGURE 8.—Circumferential pressure distribution at scroll inlet for actual tip speed of 1000 feet per second.

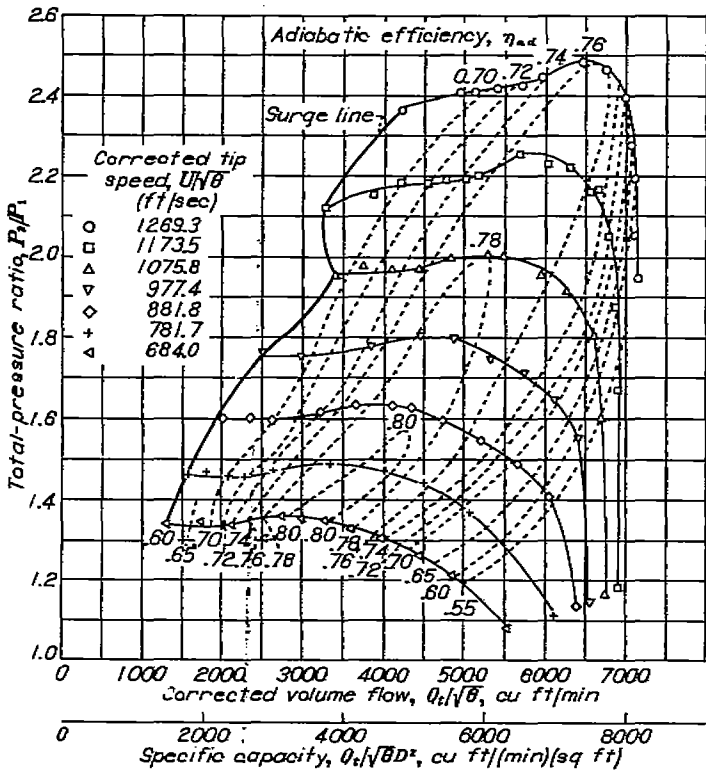


FIGURE 9.—Typical performance curves of compressor consisting of mixed-flow impeller 20-inch diffuser, and sand-cast 80° symmetrical scroll.

for this impeller followed by a collector ring; (2) the 20-inch vaneless diffuser (the same one used with the family of scrolls) followed by a collector ring; (3) the 20-inch diffuser and a diffusing scroll; and (4) a 34-inch vaneless diffuser (the same as the 20-in. except for diameter) followed by a collector ring, which permitted intercomparisons of compressor operation with various components. The over-all compressor performance with these different configurations (figs. 10 and 11) was compared for an actual tip speed of 900 feet per second because directly comparable data were available for the four compressor installations at this speed.

Substitution of the 20-inch vaneless for the vaned diffuser (both with a collector ring) results in a loss of 3 to 5 points in efficiency over most of the normal operating range (load coefficient, about 0.20 to 0.25) but postpones incipient surging to considerably lower flows and increases the maximum capacity (fig. 10). When the collector ring is replaced by a scroll, the efficiency is raised to values 8 to 12 points higher than those for the same diffuser and a collector ring, and the operating range is appreciably extended toward the high load coefficients. The 20-inch vaneless diffuser and the scroll raise the efficiency from 3 to 8 points above that for the vaned diffuser and collector ring and provide a much wider operating range. Except at the highest flows, the efficiency of the 20-inch diffuser and scroll compares well with that of the 34-inch diffuser and collector ring.

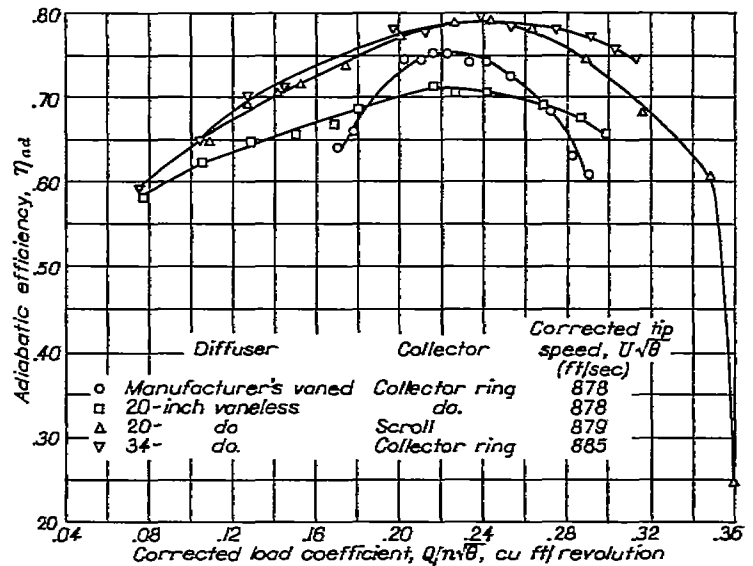


FIGURE 10.—Adiabatic efficiency of compressor consisting of mixed-flow impeller with various diffusers and collectors at actual tip speed of 900 feet per second.

Variations in pressure coefficient (fig. 11) due to changes in diffuser and collector are qualitatively similar to those in efficiency. Substitution of the 20-inch vaneless diffuser for the vaned diffuser results in a 3- to 5-point loss in pressure coefficient. Substitution of the scroll for the collector ring raises the pressure coefficient to values appreciably above those with the vaned diffuser and collector ring and to about the same values as those for the 34-inch diffuser and collector ring. Although the curves shown are for actual tip speeds, the equivalent tip speeds were nearly enough alike to allow a qualitative comparison.

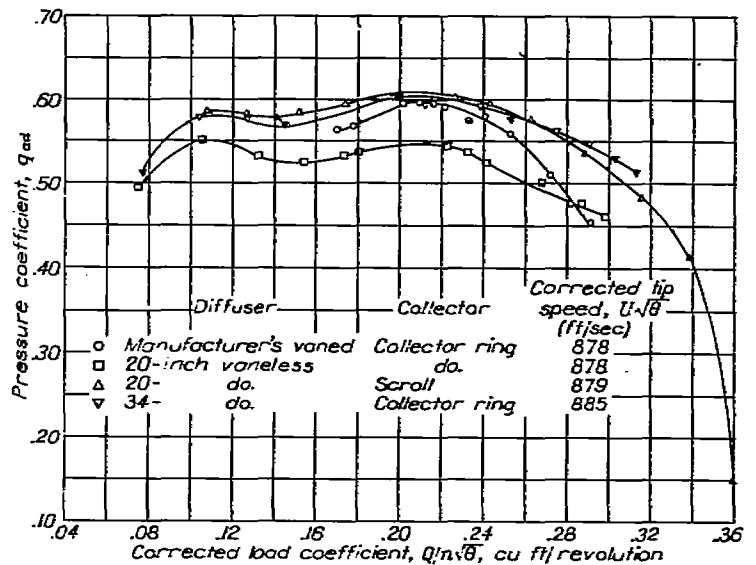


FIGURE 11.—Pressure coefficient of compressor consisting of mixed-flow impeller with various diffusers and collectors at actual tip speed of 900 feet per second.

SUMMARY OF RESULTS

A method for designing diffusing scrolls was developed and applied in the construction of a family of scrolls of different cross-sectional shapes. The scrolls were then investigated as a compressor component with an 11.24-inch-diameter mixed-flow impeller and a 20-inch-diameter vaneless diffuser. The performance of a representative scroll was then compared (for the same impeller) with that of other configurations incorporating a collector ring instead of a scroll. The following results were obtained:

1. The design method accomplished the desired circumferential uniformity of pressure at the scroll inlet under design conditions for the scrolls investigated and hence was applicable throughout the range of geometric variations employed.

2. The changes in scroll geometry and surface condition employed in this study resulted in negligible differences in compressor performance though indications exist that the 24° divergence angle is too small for optimum performance at high tip speeds.

3. Substitution of the scroll for the collector ring, both with the 20-inch diffuser, gave increases in efficiency of 3 to

12 points, substantial increases in pressure coefficient, and extended the operating range to significantly higher values of load coefficient.

4. The compressor performance with the scroll and 20-inch vaneless diffuser compared well with the performance when a collector ring was used with either a 17-inch vaned diffuser or a 34-inch vaneless diffuser.

FLIGHT PROPULSION RESEARCH LABORATORY,
NATIONAL ADVISORY COMMITTEE FOR AERONAUTICS,
CLEVELAND, OHIO, *October 1947.*

REFERENCES

1. Brown, W. Byron, and Bradshaw, Guy R.: Method of Designing Vaneless Diffusers and Experimental Investigation of Certain Undetermined Parameters. NACA TN 1426, 1947.
2. Ellerbrock, Herman H., and Goldstein, Arthur W.: Principles and Methods of Rating and Testing Centrifugal Superchargers. NACA ARR, Feb. 1942.
3. NACA Subcommittee on Supercharger Compressors: Standard Method of Graphical Presentation of Centrifugal Compressor Performance. NACA ARR E5F13a, 1945.